J|A|C|S COMMUNICATIONS

Published on Web 09/21/2009

Noncovalent Metal−Metal Interactions: The Crucial Role of London Dispersion in a Bimetallic Indenyl System

Tobias Schwabe,[†] Stefan Grimme,*[,†] and Jean-Pierre Djukic[‡]

Organisch-Chemisches Institut, Westfälische Wilhelms Universität, Corrensstrasse 40, 48149 Münster, Germany, and Institut de Chimie, Université de Strasbourg, 4 rue Blaise Pascal, 67000 Strasbourg, France

Received July 15, 2009; E-mail: grimmes@uni-muenster.de

The nature of the "heterodox bond" in bimetallic indene complexes has been investigated with high-level ab initio electronic structure methods, with a special focus on the contribution of intramolecular London dispersion effects. Their accurate account is highly relevant to the implementation of new stereoselective processes whereby weak interactions may contribute decisively to provide stereospecificity.[1] One illustrative molecular system is that of the anti- and syn-facial rhodium(I)[2] and iridium(I)[3] derivatives of tricarbonyl(η^6-indene)chromium reported by Ceccon and co-workers.[4] The syn- and anti-facial isomers differ by the position of the $Cr(CO)_3$ and ML_2 moieties relative to the plane of the indenyl ligand (Chart 1). The Cr-to-M distances are typically ∼3.1 Å in syn-facial isomers. Ceccon and co-workers showed that under particular conditions, the anti-facial isomer could convert into the thermodynamic product, i.e., the syn-facial isomer. A covalency-focused theoretical investigation[5] of this unusual positional preference in *syn*-**2** raised a major paradox: the four-electron−two-orbital nature of the "heterodox"[5] Cr−Rh interaction suggests the absence of a bond between the two metal centers. Hereafter, it is demonstrated not only that the syn-facial structures are energetically favored relative to the antifacial isomers but that this stereochemical preference is an illustration of the central role of noncovalent attractive dispersion-type forces in coordination compounds.

Chart 1. Structures of the Considered Syn- and Anti-Facial Bimetallic Indenyl Species (CSDB Reference Codes Are Given in Brackets)

anti-**1** (ZAFPAX)
anti-**2**
anti-**3** (KACHUR)
anti-**4**

syn-**1** (HAPPIX) [ML_2= Rh(*nbd*)]
syn-**2** (HAPPOD) [ML_2= $Rh(CO)_2$]
syn-**3** (YUGZUV) [ML_2= Rh(*cod*)]
syn-**4** (POYSOL) [ML_2= $Ir(CO)_2$]

nbd: norbornadiene; *cod*: cyclooctadiene

Significant dispersion interactions between (closed-shell) transition-metal fragments have been studied theoretically and seem to occur for various elements.[6] To analyze whether this also holds for the "heterodox bond",[5] quantum-chemical investigations were carried out. For four representative examples from the literature, the structures and relative energies for the co-facial (syn) and antarafacial (anti) isomers (Chart 1) were computed. All of the geometries were fully optimized. Density functional theory (DFT) was applied with the functionals BP86[7] and TPSS,[8] which are well-established standard methods for transition-metal complexes. To compensate for the inability of common functionals to describe dispersion effects correctly, the DFT-D[9] method was used as well. Finally, wave-function-based perturbation theory in its improved form, namely, spin-component-scaled MP2 (SCS-MP2),[10] was used for comparison, and a molecular-fragment-based analysis of bonding was performed. All of the computations were done with a slightly modified version of TURBOMOLE 5.9 employing large, heavily polarized triple-ζ-type Gaussian AO basis sets (def2-TZVP).[11] The following discussion will concentrate mainly on case **2**, which we consider to be a prototypical system. Analogous data were obtained for **1**, **3**, and **4** [see the Supporting Information (SI)]. Because the BP86 and TPSS functionals provide very similar results, only the results obtained using the latter are discussed.

Table 1. Characteristic Distances (pm) for *syn*-**2** and *anti*-**2**

	method	Cr−Rh	Cr−C10	Cr−C1	Rh−C1	Rh−C8
syn	TPSS	309.7	183.5	238.8	259.6	217.7
	TPSS-D	308.5	183.4	237.2	259.9	216.4
	SCS-MP2	296.7	173.7	236.7	248.8	213.7
	exptl	307.7	181.4	240.1	254.2	218.9
anti[a]	TPSS	454.9	184.4	228.4	249.2	222.8
	TPSS-D	446.6	184.4	225.7	244.1	222.9
	SCS-MP2	435.4	176.7	221.9	237.1	221.3

[a] No experimental data available.

In Table 1, some representative structural data for *syn*-**2** are shown (see Figure 1 for definitions) and compared with corresponding experimental values. In general, the DFT methods [also BP86(-D); see the SI] describe the systems fairly well. With TPSS, the metal−metal distance is overestimated by ∼2 pm, an error which is reduced to 0.8 pm by the dispersion correction. The difference between TPSS and TPSS-D is even larger for the anti form (7.3 pm). As expected, SCS-MP2 systematically yields M−ligand bond lengths that are too short. The magnitude and direction of the semiclassical dispersion correction (i.e., TPSS vs TPSS-D) in both forms are consistent with the picture that rather long-range L−L interactions are mainly important; however, this yields no decisive answer to the question of "heterodox" bonding, particularly in regard to the role of the metal centers. An interesting picture comes from the relative energies of the syn and anti forms (Table 2). Except for the TPSS results in case **3**, the syn isomers are always lower than the anti forms at correlated theoretical levels. This is in qualitative agreement with the experimental observations. The syn form is more favored by the dispersion correction, and thus, the corresponding TPSS-D values are in better agreement with the SCS-MP2 results than are the TPSS (or BP86) values. For the bulkier *cod* ligand (**3**), uncorrected functionals fail to describe the preference for the syn isomer correctly. This observation leads to the conclusion that dispersion between the ligands is also a relevant part of the stabilization of the syn isomers.[12]

The nature of the metal−metal interaction was characterized in more detail using a relatively new analysis procedure.[13] This

[†] Westfälische Wilhelms Universität.
[‡] Université de Strasbourg.

10.1021/ja905617g CCC: $40.75

procedure has previously been successfully used to study intramolecular interactions in (bio)organic molecules[13a,b] and to reveal the aurophilic effect.[13c] A similar approach with fragment molecular orbitals was also proposed.[13d] In the present study, SCS-MP2 calculations were performed in a localized molecular orbital (LMO) basis that was obtained with the Pipek−Mezey[14] algorithm.

Table 2. Relative (Zero-Point Vibrational Energy Exclusive) Energies ΔE(syn−anti) = E(syn) − E(anti) for Complexes **1**−**4** (kcal mol^{-1})

case	HF[a]	TPSS	TPSS-D	SCS-MP2
1	+14.3	−2.3	−8.6	−5.6
2	+10.9	−2.5	−7.3	−4.5
3	+15.3	+0.3	−6.9	−3.6
4	+14.1	−3.5	−8.8	−5.7

[a] SCS-MP2/def2-TZVP geometries.

Each occupied orbital was assigned to one fragment of the system (see Figure 1 for definitions) on the basis of the atoms on which it is localized. For ambiguous cases (e.g., M−indenyl), the respective orbitals were always assigned to the metal fragments. The number of orbitals in each fragment is the same for the syn and anti isomers. This LMO-SCS-MP2 approach allows a convenient partitioning of the correlation energy into orbital pairs (for details, see the SI). In a second step, the differences in the intra- and interfragment-pair correlation energies for the syn−anti conformational process were calculated; their sum is the total SCS-MP2 correlation energy contribution to ΔE(syn−anti). At the Hartree−Fock level, the anti form is always incorrectly computed to be much lower in energy (Table 2), which shows that the discussed effect is entirely due to electron correlation.

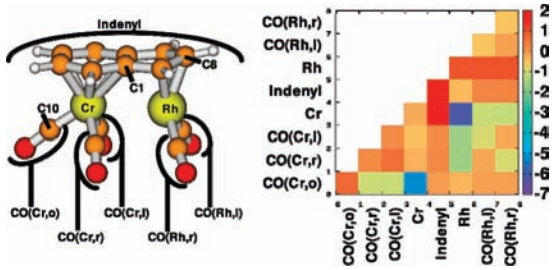

Figure 1. Differences in intrafragment (diagonal entries) and interfragment (off-diagonal entries) correlation energies (kcal mol^{-1}) between *syn*-**2** and *anti*-**2** at the SCS-MP2 level.

The results of the fragment-based analysis for *syn*-**2** and *anti*-**2** are depicted in Figure 1 in color-coded matrix form. In this matrix, the differences in intrafragment correlation energies can be found along the diagonal. As expected, these values are rather small because the shapes of the orbitals are similar for the two conformers. The two largest (stabilizing) contributions originate from a more favorable electron correlation between the outer CO ligand and Cr and between the metal centers themselves. This latter contribution arises from simultaneous (single) excitations of one electron localized near Cr and a second electron on Rh. Such excitations are typical for dispersive interactions. In agreement with the DFT-D results, additional stabilizing correlations are found between the ligands of different metal centers as well as between ligands on the same metal center. By far the largest syn-stabilizing contribution comes from the metals. The effect increases for heavier metals: e.g., in going from Rh to Ir (see the SI), the corresponding Cr−M interfragment contribution increases to −11.0 kcal mol^{-1} (M = Ir, *syn*-**4**) from −6.1 kcal mol^{-1} (M = Rh, *syn*-**2**). This increase is consistent with the interpretation that the preferred syn conformation is a consequence of a dispersion effect (higher polarizability of Ir). The phenomenon seems to be akin to metallophilicity, which is typical for heavy late transition metals. A similar bonding situation for 3d transition metals is thus demonstrated for the first time by the LMO-SCS-MP2 analysis. Previous DFT-D investigations of a Cr−Mn system[15] merely assumed the role of dispersion.

In conclusion, we have shown that there are two separable nonlocal correlation (London dispersion) effects, ligand−metal and ligand−ligand, as well as the surprisingly strong metal−metal interaction, that are responsible for the "heterodox bonding"[5] in bimetallic indenyl complexes. Although the latter can be described to some extent by conventional density functionals because of the intermediate M−M distance (and concomitantly significant overlap density), these methods do not sufficiently account for the intramolecular ligand−ligand effects. This emphasizes that the use of "dispersion-including" DFT methods should be generalized and not limited to biomolecules. On the positive side, a deeper understanding of these so-called medium-range dispersion effects[16] (which are typically operative between 250 and 350 pm) can lead to more rational design principles in organometallic chemistry.

Acknowledgment. The Fonds der Chemischen Industrie, the Centre National de la Recherche Scientifique, and the A. von Humboldt Stiftung are kindly acknowledged for their support.

Supporting Information Available: Complete ref 11c; computational details, structural data, and total and relative energies of **1**−**4** with BP86(-D), TPSS(-D), and SCS-MP2; TPSS-D geometries for all structures; theoretical background of correlation energy partitioning and "heterodox" bonds; and LMO-SCS-MP2 results for the fragment analyses of **1**, **3**, and **4**. This material is available free of charge via the Internet at http://pubs.acs.org.

References

(1) (a) Knowles, J. R. *Nature* **1991**, *350*, 121. (b) Sabo-Etienne, S.; Chaudret, B. *Mod. Coord. Chem.* **2002**, 45. (c) Shinisha, C. B.; Sunoj, R. B. *Org. Biomol. Chem.* **2008**, *6*, 3921.
(2) (a) Ceccon, A.; Gambaro, A.; Santi, S.; Valle, G.; Venzo, A. *J. Chem. Soc., Chem. Commun.* **1989**, 51. (b) Bonifaci, C.; Ceccon, A.; Gambaro, A.; Ganis, P.; Santi, S.; Valle, G.; Venzo, A. *Organometallics* **1993**, *12*, 4211. (c) Bonifaci, C.; Ceccon, A.; Gambaro, A.; Ganis, P.; Santi, S.; Venzo, A. *Organometallics* **1995**, *14*, 2430. (d) Bonifaci, C.; Carta, G.; Ceccon, A.; Gambaro, A.; Santi, S.; Venzo, A. *Organometallics* **1996**, *15*, 1630. (e) Mantovani, L.; Ceccon, A.; Gambaro, A.; Santi, S.; Ganis, P.; Venzo, A. *Organometallics* **1997**, *16*, 2682.
(3) Cecchetto, P.; Ceccon, A.; Gambaro, A.; Santi, S.; Ganis, P.; Gobetto, R.; Valle, G.; Venzo, A. *Organometallics* **1998**, *17*, 752.
(4) Bonifaci, C.; Ceccon, A.; Gambaro, A.; Manoli, F.; Mantovani, L.; Ganis, P.; Santi, S.; Venzo, A. *J. Organomet. Chem.* **1998**, *577*, 97.
(5) Bonifaci, C.; Ceccon, A.; Santi, S.; Mealli, C.; Zoellner, R. W. *Inorg. Chim. Acta* **1995**, *240*, 541.
(6) Pyykkö, P. *Chem. Rev.* **1997**, *97*, 597.
(7) (a) Becke, A. D. *Phys. Rev. A* **1988**, *38*, 3098. (b) Perdew, J. P. *Phys. Rev. B* **1986**, *33*, 8822.
(8) Tao, J.; Perdew, J. P.; Staroverov, V. N.; Scuseria, G. E. *Phys. Rev. Lett.* **2003**, *91*, 146401.
(9) Grimme, S. *J. Comput. Chem.* **2006**, *27*, 1787.
(10) Grimme, S. *J. Chem. Phys.* **2003**, *118*, 9095.
(11) (a) Weigend, F.; Ahlrichs, R. *Phys. Chem. Chem. Phys.* **2005**, *7*, 3297. (b) Weigend, F.; Häser, M.; Patzelt, H.; Ahlrichs, R. *Chem. Phys. Lett.* **1998**, *294*, 143. (c) Ahlrichs, R.; et al. *TURBOMOLE*, version 5.9; Universität Karlsruhe: Karlsruhe, Germany, 2006. (d) Weigend, F. *Phys. Chem. Chem. Phys.* **2006**, *8*, 1057. (e) Hellweg, A.; Hättig, C.; Höfener, S.; Klopper, W. *Theor. Chem. Acc.* **2007**, *117*, 587.
(12) Orian, L.; Hanis, P.; Santi, S.; Ceccon, A. *J. Organomet. Chem.* **2005**, *690*, 482.
(13) (a) Grimme, S.; Mück-Lichtenfeld, C.; Antony, J. *Phys. Chem. Chem. Phys.* **2008**, *10*, 3327. (b) Wiberg, K. B.; Wang, Y.; Petersson, G. A.; Bailey, W. F. *J. Chem. Theory Comput.* **2009**, *5*, 1033. (c) Runeberg, N.; Schütz, M.; Werner, H.-J. *J. Chem. Phys.* **1999**, *110*, 7210. (d) Ishikawa, T.; Mochizuki, Y.; Amari, S.; Nakano, T.; Tokiwa, H.; Tanaka, S.; Tanaka, K. *Theor. Chem. Acc.* **2007**, *118*, 937.
(14) Pipek, J.; Mezey, P. G. *J. Chem. Phys.* **1989**, *90*, 4916.
(15) Hyla-Kryspin, I.; Grimme, S.; Djukic, J. P. *Organometallics* **2009**, *28*, 1001.
(16) (a) Grimme, S. *Angew. Chem., Int. Ed.* **2006**, *45*, 4460. (b) Grimme, S. *Chem.—Eur. J.* **2004**, *10*, 3423.

JA905617G